Synthesis and Spectroscopic Characterization of a Zeolite-Entrapped $Ru(bpy)_2(dpp)^{2+}$ Complex

Anwar A. Bhuiyan and James R. Kincaid*

Chemistry Department, Marquette University, Milwaukee, Wisconsin 53201-1881

Received March 31, 1999

The heteroleptic ruthenium(II) complex $Ru(bpy)_2(dpp)^{2+}$ (where bpy = 2,2′-bipyridine and dpp = 2,3-bis(2-pyridyl)pyrazine) has been prepared in the supercages of Y-zeolite and characterized by diffuse reflectance, electronic absorption, electronic emission, and resonance Raman (RR) spectroscopy, as well as lifetime measurements. The spectral results confirm the identity of the entrapped complex. The diffuse reflectance spectrum of the zeolite-entrapped complex is slightly red-shifted in the visible region compared to the absorption spectrum of the free complex in water solution. The emission maximum for the zeolite-entrapped complex is red-shifted by 16 nm with respect to the complex in water solution and by 38 nm relative to the complex in acetonitrile solution. The emission maximum for a zeolite surface-adsorbed complex is blue-shifted by 12 nm with respect to the complex in water solution, but the emission maxima of the liberated complex after dissolution of the zeolite matrix, for both the entrapped and adsorbed complexes, are identical to the spectrum of the free complex in water solution. There are moderate RR frequency shifts observed for the zeolite-entrapped complex relative to the solution-phase complex as a consequence of the interaction of the complex with the zeolite framework. The excited state lifetime measurement shows no dramatic changes upon entrapment within the zeolite supercages. Temperature-dependent lifetime measurements indicate that the excited state decays via two thermally accessible upper states.

Introduction

In an effort to develop synthetic systems for the effective capture and utilization of solar solar energy,[1−3] the zeolite-entrapped polypyridine complexes of divalent ruthenium have attracted much attention.[4−8] This demonstrated potential has prompted us to embark on a systematic investigation of the effects of the zeolite framework on the inherent photophysical properties of the entrapped complexes.[8−14] Following the impressive work by Dutta and co-workers,[6,7,15] which documented efficient photoinduced electron transfer from entrapped $Ru(bpy)_3^{2+}$ to intrazeolitic acceptors, we described a synthetic strategy for the preparation of zeolite-based molecular assemblies composed of donor−acceptor−sensitizer triads entrapped in adjacent supercages of Y-zeolite and demonstrated a dramatic (4-fold) increase in observed charge-separation efficiency.[8]

These encouraging results have prompted us to explore synthetic schemes for the construction of covalently linked zeolite-based molecular assemblies. This task can be accomplished by using bridging ligands, such as 2,3-bis(2-pyridyl)-pyrazine (dpp), which are capable of linking the components. Complexes based on dpp are a natural starting point because of its commercial availability and the well-documented photophysics of such systems.[16]

In this paper, we report efficient synthetic methods for the preparation of the zeolite-entrapped $Ru(bpy)_2(dpp)^{2+}$ complex (shown in Figure 1). Spectroscopic and photophysical studies confirm the structural integrity of the complex and document the fact that its inherently favorable photophysical properties are not substantially altered by the zeolite framework.

Experimental Section

A. Materials. The Y-zeolite, the ligands, 2,2′-bipyridine (bpy) and 2,3-bis(2-pyridyl) pyrazine (dpp), $RuCl_3 \cdot 3H_2O$, $Ru(NH_3)_6Cl_3$, and $NaClO_4$ were purchased from the Aldrich Chemical Co., Milwaukee, WI. The calcined zeolite sample[17] was extensively washed with a 10% NaCl solution and then deionized water. The ligands were sublimed prior to use, and the other chemicals were used without further purification. All solvents used were reagent grade or better.

B. Preparation of Compounds. The zeolite-entrapped complex $Z-Ru(bpy)_2(dpp)^{2+}$ was prepared in two steps by a modification of a method previously developed in our laboratory,[9,14] which is based on pioneering work of Lunsford and co-workers.[18,19] In the first step, a water suspension (pH = 5.5) of calcined zeolite (2.0 g) was ion-exchanged overnight at 4 °C with the appropriate amount of $Ru(NH_3)_6Cl_3$ (depending on the desired load of the complex, such as 5 mg for

(1) Parmon, V. N.; Zamarev, K. I. In *Photocatalysis: Fundamentals and Applications;* Serpone, N., Pelizzetti, E., Eds.; Wiley: New York, 1989; p 565.
(2) Kalyanasundaram, K. *Photochemistry in Microheterogeneous Systems;* Academic Press: New York, 1987.
(3) Gratzel, M., Ed. *Energy Resources Through Photochemistry and Catalysis*; Academic Press: New York, 1983.
(4) Ramamurthy, V., Ed. *Photochemistry in Organized and Constrained Media*; VCH: New York, 1991.
(5) Persayd, L.; Bard, A. J.; Campion, A.; Mallouk, T. E.; Webber, S. E.; White, J. M. *J. Am. Chem. Soc.* **1987**, *109*, 7309.
(6) Dutta, P. K.; Ledney, M. *Prog. Inorg. Chem.* **1997**, *44*, 209.
(7) Borja, M.; Dutta, P. K. *Nature* **1993**, *362*, 43.
(8) Sykora, M.; Kincaid, J. R. *Nature* **1997**, *387*, 162.
(9) Maruszewski, K.; Strommen, D. P.; Handrich, K.; Kincaid, J. R. *Inorg. Chem.* **1991**, *30*, 4579.
(10) Maruszewski, K.; Strommen, D. P.; Kincaid, J. R. *J. Am. Chem. Soc.* **1993**, *115*, 8345.
(11) Maruszewski, K.; Kincaid, J. R. *Inorg. Chem.* **1995**, *34*, 2002.
(12) Szulbinski, W. S.; Kincaid, J. R. *Inorg. Chem.* **1998**, *37*, 859.
(13) Bhuiyan, A. A.; Kincaid, J. R. *Inorg. Chem.* **1998**, *37*, 2525.
(14) Sykora, M.; Maruszewski, K.; Treffert-Ziemelis, S. M.; Kincaid, J. R. *J. Am. Chem. Soc.* **1998**, *120*, 3490.
(15) Dutta, P. K.; Turbeville, W. *J. Phys. Chem.* **1992**, *96*, 9410.
(16) Kalyanasundaram, K.; Nazeeruddin, M. K. *Inorg. Chem.* **1990**, *29*, 1888.
(17) Incavo, J. A.; Dutta, P. K. *J. Phys. Chem.* **1990**, *94*, 3075.
(18) DeWilde, W.; Peeters, G.; Lunsford, J. H. *J. Phys. Chem.* **1980**, *84*, 2306.
(19) Quayle, W. H.; Lunsford, J. H. *Inorg. Chem.* **1982**, *21*, 97.

10.1021/ic990359s CCC: $18.00 © 1999 American Chemical Society
Published on Web 09/16/1999

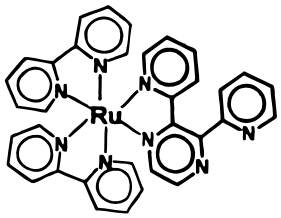

Figure 1. Schematic representation of the $Ru(bpy)_2(dpp)^{2+}$ complex.

1 complex per 60 supercages). The filtered, dried solid ($Z-Ru(NH_3)_6^{3+}$) was suspended in ~10 mL of ethanol, and a 50-fold excess of bpy ligand (with respect to $Ru(NH_3)_6^{3+}$) was added and soaked overnight at 4 °C. The suspension was then transferred to a Pyrex vacuum reaction tube, and the ethanol was evaporated under a stream of nitrogen.The evacuated tube was then partially immersed in an oil bath and heated at 90 °C for 18 h. The product was washed as described previously[15] and then extensively (~15 days) Soxhlet-extracted with 95% ethanol to remove the excess ligand (as confirmed by the ultraviolet absorption spectrum of the ethanol washing). Spectroscopic measurements documented the formation of $Z-Ru(bpy)_2(H_2O)_2^{2+}$, which was then used as the precursor material for the preparation of $Z-Ru(bpy)_2(dpp)^{2+}$. In the second step, a 100-fold molar excess of dpp ligand (with respect to the entrapped $Ru(bpy)_2^{2+}$) was added to the $Z-Ru(bpy)_2^{2+}$ and the sample was mechanically mixed well in the solid state and then transferred to the reaction tube. The sample was evacuated and heated as described above with the exception that the oil bath was maintained ~200 °C for 48 h and then allowed to cool to room temperature. Another portion (20-fold excess) of dpp was added. After evacuation (three times), the tube was heated again for an additional 24 h. The sample was purified as described above. The zeolite-entrapped complex was extracted from the zeolite matrix by the hydrofluoric acid method described in ref 9. The integrity of the zeolite-entrapped sample was confirmed by the spectroscopic measurements.

The free complexes $Ru(bpy)_2Cl_2$ and $Ru(bpy)_2(dpp)ClO_4$ were prepared by literature methods.[20,21] The final sample was purified by repeated recrystallization from 1:1 water−ethanol solutions and further purified on a silica gel column, which was eluted with a 0.5 M ethanolic solution of $(C_2H_5)_4NBr$.

The zeolite surface-adsorbed complex was prepared by a slight modification of literature methods.[11,22] Briefly, the pH of a water suspension of calcined zeolite (1.0 g) was adjusted to ~5.5 and then the appropriate amount of $Ru(bpy)_2(dpp)(ClO_4)_2$ (resulting in a 10^{-5} M aqueous solution of $Ru(bpy)_2(dpp)(ClO_4)_2$) was added and the mixture was stirred for ~2 h. The zeolite sample was then filtered off, repeatedly washed with deionized water, and dried under air.

C. Spectroscopic Measurements. 1. Electronic Absorption Spectra. Electronic absorption spectra were obtained with a Hewlett-Packard model 8452A diode array spectrometer using a 1-cm quartz cuvette. Spectra were obtained in the absorbance mode. The diffuse reflectance spectra were recorded on a Shimadzu 2501 scanning spectrometer equipped with a Shimadzu integrating sphere attachment. The samples were measured as KBr pellets. For these measurements, a calcined plain Na−Y-zeolite sample was used as a blank and finely ground $BaSO_4$ was used as a reference. The spectra were recorded in the transmittance mode and then numerically Kubelka−Munk[23] corrected using SpectraCalc software.

2. Resonance Raman Spectra. Spectra were obtained with a Spex model 1403 double monochromator equipped with a Spex model DM1B controller and a Hamamatsu R928 photomultiplier tube. The excitation lines 488.0 and 457.9 nm were obtained from a Spectra-Physics model 2025-05 argon ion laser, and the 413.1 nm excitation line was obtained from a Coherent Innova 100-K3 krypton ion laser. Spectra of the zeolite-entrapped compound were obtained from solid samples in a rotating NMR tube. Spectra of the free complex and the complex extracted from the zeolite matrix were obtained from aqueous solutions. The absorption spectra were the same before and after RR measurements, indicating that there was no significant photodecomposition upon exposure to laser excitation. The spinning 5 mm i.d. NMR tube was illuminated by a laser beam focused through a glass lens, and the scattered light was collected with a conventional two-lens collection system.

3. Electronic Emission Spectra. The spectroscopic apparatus was the same as that for the Raman measurements, using the 488.0 nm excitation from a Spectra-Physics model 2025−05 argon ion laser. Spectra of the zeolite-entrapped complex were obtained from solid samples in a rotating NMR tube. The spinning 5 mm i.d. NMR tube was illuminated by a laser beam focused through a glass lens (laser power ~10 mW at the sample), and the emission from the sample was collected with a conventional two-lens collection system. Spectra of the compound extracted from the zeolite matrix were obtained from a water solution, and those of the free complex were obtained in acetonitrile or water solution.

4. Excited State Lifetimes. The zeolite-entrapped complex used for the lifetime measurements was degassed overnight at $\sim 10^{-4}$ Torr and then exposed to the vapors of degassed (three freeze−pump−thaw cycles) deionized water. The liquid samples were degassed by three freeze−pump−thaw cycles and then sealed inside the NMR tube on the vacuum line. The third harmonic (354.7 nm) of a Quanta-Ray (Spectra-Physics) model GCR-11 Nd:YAG laser (operated at 20 Hz), with the beam defocused, was used as the excitation source for the lifetime measurements. The emitted light from the sample was transferred through collecting and transferring lenses to a Spex 340S spectrometer equipped with an RCA C31034A-02 photomultiplier tube with an applied voltage of 1800 V. The photomultiplier tube output signal was directed to a Lecroy 9450A dual 300 MHz oscilloscope. The emission was monitored at 700 nm for the zeolite-entrapped complex and at 684 or 662 nm for the free complex in aqueous or acetonitrile solution, respectively. In all cases, 3000 scans of the emission decay curves were averaged and transferred to the computer. The emission decay curves were then fitted to a mono- or biexponential model using commercial software (PSI-Plot) based on the Marquardt−Levenberg algorithm.[24]

The temperature-dependent lifetime measurements were acquired with the aid of a cold cell of in-house design, which consists of a Dewar flask containing an NMR tube spinner. Prior to the measurement, the samples were degassed as mentioned before. For the low-temperature measurement, the Dewar flask was filled with an ethanol/liquid nitrogen cooling mixture, and an NMR tube containing the samples was then immersed. The sample temperature was allowed to equilibrate for at least 5 min while the NMR tube was spinning to prevent local overheating and possible decomposition of the complex. The temperature of the cooling mixture was allowed to rise slowly, and the decay curves were measured at various temperatures. The temperature inside the Dewar flask was measured using a TEGAM 821 microprocessor thermometer equipped with thermocouple. The temperature variations during the collection of the data (500 sweeps/25 s) were approximately 0.5−0.6 °C. The average value was considered as the experimental temperature for the measurement. The measurements at temperatures above 20 °C were taken with the same setup using hot water as the heating liquid. The sample was first immersed in boiling water, and decay curves then were measured at various temperatures as the water bath was allowed to cool.

Results and Discussion

A. Synthesis. The emission spectrum of the zeolite-entrapped complex shows a very weak shoulder (at ~610 nm) on the blue side of the main emission band resulting from the presence of a trace amount (<1%) of tris-ligated species, $Z\text{-}Ru(bpy)_3^{2+}$. Several variations in the procedure for the preparation of pure complex were investigated. It was determined that the tris

(20) Sprintschnik, G.; Sprintschnik, H. W.; Krisch, P. P.; Whitten, D. G. *J. Am. Chem. Soc*. **1977**, *99*, 4947.
(21) Braunstein, C. H.; Baker, A. D.; Strekas, T. C.; Gafney, H. D. *Inorg. Chem.* **1984**, *23* 857.
(22) Kim, Y.; Mallouk, T. E. *J. Phys. Chem*. **1992**, *96*, 2879.
(23) Kubelka, P. *J. Opt. Soc. Am*. **1948**, *38*, 448.
(24) Marquardt, D. W. *J. Soc. Ind. Appl. Math*. **1963**, *11*, 431.

impurities were formed during the 90 °C heating for the preparation of bis-homoleptic complex $Z-Ru(bpy)_2^{2+}$, as evidenced by slight luminescence of the sample of the bis complex (~620 nm). The pure bis complex, $Z-Ru(bpy)_2(H_2O)_2^{2+}$, does not emit strongly at room temperature, but the tris-ligated complex, $Z-Ru(bpy)_3^{2+}$, emits at ~620 nm. Some time and effort were expended in developing proper conditions to prevent formation of the $Z-Ru(bpy)_3^{2+}$ impurity. In some cases, samples were heated at 90 °C for long periods (up to several days), and then, after washing, the emission spectra were measured and showed slight luminescence at ~620 nm. Though formation of the $Z-Ru(bpy)_3^{2+}$ impurity cannot be entirely prevented, it was found that 18 h of heating at 90 °C are the best conditions to minimize the level of impurity. The sample of zeolite-entrapped bis complex used here contained less than 1% of the tris complex impurities, as determined with emission spectroscopy by spiking the samples of $Z-Ru(bpy)_2^{2+}$ with small (known) amounts of $Z-Ru(bpy)_3^{2+}$. The $Z-Ru(bpy)_2(dpp)^{2+}$ complex also contains less than 1% $Z-Ru(bpy)_3^{2+}$ impurity as determined by the same procedure.

B. Electronic Absorption and Emission Spectra. The diffuse reflectance spectrum of the zeolite-entrapped $Ru(bpy)_2dpp^{2+}$ complex exhibits absorption maxima at 284, 430, and 474 nm. The absorption spectrum of the free complex in water solution matches that reported in the literature.[16] The diffuse reflectance spectrum of the zeolite-entrapped complex shows slight red shifts in the positions of the absorption maxima in the visible region compared to the spectrum of the free complex in water solution. The absorption spectrum of the liberated complex after dissolution of the zeolite matrix is identical to the spectrum of the free complex in water solution. The absorption spectra of such complexes consist of a series of absorption bands in the UV and visible regions. The intense UV bands are ascribable to ligand-centered $\pi-\pi^*$ transitions.[25,26] The visible spectrum is not well resolved and consists of absorption bands at ~430 and ~479 nm. The visible bands are assigned to $d-\pi^*$ MLCT transitions.[16,25,26] The lower energy band is assigned to a Ru → dpp transition, and the higher energy one is ascribable to a Ru → bpy transition.[21] These assignments are confirmed by selective enhancement of ligand-specific resonance Raman bands at various excitation wavelengths (vide infra).

The emission spectrum of the zeolite-entrapped complex shows a very weak shoulder (~610 nm), attributable to a trace amount (<1%) of $Z-Ru(bpy)_3^{2+}$, and a strong emission band with a maximum at 700 nm. The emission maximum (700 nm) observed for the $Z-Ru(bpy)_2(dpp)^{2+}$ complex is red-shifted from that observed for the free complex (662 nm in acetonitrile and 684 nm in water) at room temperature. The emission maximum (672 nm) observed for the zeolite surface-adsorbed complex is blue-shifted by 12 nm with respect to that of the free complex in water solution. The emission spectra of the free complex are in good agreement with the previously reported spectra.[16] The emission spectra of the HF extracts obtained from dissolution of the zeolite matrix, for both the entrapped and adsorbed complexes, are superimposable on that of the free complex in water, except for the appearance of a weak shoulder at ~610 nm in the case of the zeolite-entrapped complex, which is associated with the $Ru(bpy)_3^{2+}$ impurity.

The red shift in the emission maximum of the zeolite-entrapped complex is somewhat surprising. For many similar complexes bearing nitrogen atoms at the ring periphery, including the surface-adsorbed $Ru(bpy)_2dpp^{2+}$ material studied here, interaction with the zeolite framework produces a blue shift in the emission maxima between ~10 and 30 nm.[10,12] The most reasonable explanation is that the rigid zeolite framework imposes structural constraints on the bulky (three-ring) dpp ligand, apparently inducing conformational changes which give rise to the lowered emission in energy. As for other polypyridine complexes of Ru(II), this luminescence is characteristic of a triplet metal to ligand charge transfer (^{3}MLCT) level, and in this specific mixed-ligand complex, luminescence is assigned to a $p\pi^*(dpp) \rightarrow d\pi(Ru)$ transition.[27−29]

C. Resonance Raman (RR) spectra. The vibrational frequencies observed in the RR spectra of the free complex are in good agreement with the literature (maximum difference of 4 cm^{-1}).[21,30] There are only moderate frequency shifts (≤ 9 cm^{-1}), mainly to higher frequency, observed for the zeolite-entrapped complex, relative to the bands for the solution-phase complex obtained here (Table 1). The spectrum of the liberated complex after dissolution of the zeolite matrix is virtually identical to that of the free complex, a fact which confirms that there is no permanent modification of the parent compound and that the frequency shifts are a consequence of the different environments. The maximum frequency shifts for the zeolite surface-adsorbed complex are ± 3 cm^{-1} relative to those of the free complex in water solution.

The spectra of the $Ru(bpy)_2(dpp)^{2+}$ complex consist of bpy vibrations as well as dpp vibrations. The bpy vibrations can easily be identified by comparison with the well-documented spectrum of $Ru(bpy)_3^{2+}$ complex[31] (Table 1). The additional vibrations at 1266, 1473, and 1519 cm^{-1} were assigned to the dpp ligand in previous reports.[21,30] In addition to those three bands, there are more dpp bands which overlap with the bpy bands. As in the case of previously studied pyridylpyrazine complexes[12,32] (Table 1), dpp vibrations consist of three subsets. One set of bands (such as 1603 and 1170 cm^{-1}) is associated with the pyridine fragment of the dpp ligand whose bands overlap the bpy bands; a second set (such as 1519 and 1473 cm^{-1}) is associated with the pyrazine fragment of the dpp ligand which has frequencies quite similar to those of coordinated bipyrazine (Table 1). A third set of vibrations have contributions from both fragments (such as 1319 and 1260 cm^{-1}) and are attributed to the inter-ring and adjacent bond stretching.

Resonance Raman spectra of the $Ru(bpy)_2(dpp)^{2+}$ complex were measured at 488.0, 457.9, and 413.1 nm excitation wavelengths. The RR spectra exhibit a revealing dependence on the excitation wavelength. The visible absorption spectrum of $Ru(bpy)_2(dpp)^{2+}$ consists of bands at ~424 and ~476 nm. Excitation (488.0 nm) within the lower energy MLCT transition selectively enhances dpp modes relative to bpy modes (1519 vs 1492 cm^{-1}). On the other hand, excitation (413.1 nm) in near resonance with the higher energy MLCT transition results in strong enhancement of the bpy modes.

(25) Wallace, A. W.; Murphy, W. R.; Petersen, J. D. *Inorg. Chim. Acta* **1989**, *166*, 47.
(26) Denti, G.; Campagna, S.; Sabatino, L.; Serroni, S.; Ciano, M.; Balzani, V. *Inorg. Chem.* **1990**, *29*, 4750.
(27) Juris, A.; Balzani, V.; Barigelletti, F.; Campagna, S.; Belser, P.; Von Zelewsky, A. *Coord. Chem. Rev.* **1988**, *84*, 85.
(28) Fuchs, Y.; Lofters, S.; Dieter, T.; Shi, W.; Morgan, R.; Strekas, T. C.; Gafney, H. D.; Baker, A. D. *J. Am. Chem. Soc.* **1987**, *109*, 2691.
(29) Kalyanasundaram, K.; Gratzel, M.; Nazeeruddin, M. K. *J. Chem. Soc., Dalton Trans.* **1991**, 343.
(30) Knorrs, C.; Gafney, H. D.; Baker, A. D.; Braunstein, C.; Strekas, T. C. *J. Raman Spectrosc.* **1983**, *14*, 32.
(31) Danzer, G.; Kincaid, J. R. *J. Phys. Chem.* **1990**, *94*, 3976.
(32) Danzer, G.; Golus, J.; Kincaid, J. R. *J. Am. Chem. Soc.* **1993**, *115*, 8643.

Table 1. Comparison of Resonance Raman Frequencies (cm^{-1}) of Zeolite-Entrapped and Aqueous Ru(II) Polypyridine Complexes Obtained with Various Excitations[a]

$Ru(bpy)_3^{2+}$ [b]		$Ru(bpz)_3^{2+}$ [b]		$Ru(pypz)_3^{2+}$ [c]	$Ru(bpy)_2(pypz)^{2+}$ [d]		$Ru(bpy)_2(dpp)^{2+}$ [e]		
Z	H_2O	Z	H_2O	H_2O	Z	H_2O	Z	H_2O	$\Delta\nu$
1611	1608	1593	1596	1606	1612	1608	1615	1610	+5
1564	1563	1517	1517	1596		1597	1610	1603	+7
1493	1491	1483	1486	1567	1565	1566	1604	1599	+5
1322	1320	1408	1410	1516	1513	1513	1572	1569	+3
1273	1276	1338	1346	1489	1488	1487	1563	1564	−1
1179	1176	1276	1277	1445	1336	1334	1518	1519	−1
1048	1043	1195	1194	1411	1275	1273	1497	1492	+5
1032	1028	1167	1164	1335	1173	1174	1479	1473	+6
672	668	1054	1051	1275	1035	1034	1414	1406	+8
		1026	1028	1182			1317	1319	−2
		802	802	1170			1273	1275	−2
		676	679	1061			1260	1266	−6
		663	666	1053			1176	1170	+6
				785			1037	1032	+5
				681			673	671	+2
				662					
				647					

[a] Z = zeolite-entrapped; H_2O = aqueous solution; $\Delta\nu = \nu$(zeolite) − ν(aqueous solution). [b] Data from ref 10. [c] Data from ref 32. [d] Data from ref 12. [e] Data from this study.

Excitation with 457.9 nm, which is intermediate between the absorption bands, moderately enhances both bpy and dpp bands.

The moderate frequency shifts observed upon entrapment of the complex into the zeolite matrix are most reasonably ascribed to the interaction of the complex with the zeolite framework. The most significant zeolite-induced frequency shifts are observed for dpp vibrational modes shown in Table 1. As can be seen, the largest changes are observed for modes at 1603 cm^{-1} (+7 cm^{-1}), 1473 cm^{-1} (+6 cm^{-1}), 1406 cm^{-1} (+8 cm^{-1}), 1266 cm^{-1} (−6 cm^{-1}), and 1170 cm^{-1} (+6 cm^{-1}), which belong to dpp vibrations, as determined by the fact that these features are more strongly enhanced with excitation within the low-energy absorption band. The 1603 cm^{-1} mode is attributable to overlap of a mode of coordinated bipyridine (1603 cm^{-1}) with that of the pyridine fragment of the dpp ligand (1596 cm^{-1}). The significant shifts probably arise as a result of the steric constraints imposed upon the three-ring dpp ligand and, to some extent, of the interaction of the peripheral nitrogen lone pairs with the zeolite framework.

D. Lifetime Measurement. The lifetimes of the complex in various forms were measured at room temperature, and the emission decay curves are shown in Figure 2. The emission was monitored at 662 nm for the free complex in acetonitrile solution, at 684 nm for the free complex in water solution, and at 700 nm for the zeolite-entrapped complex. The insert in Figure 2 presents the logarithmic plots for the same data. Trace A (in acetonitrile) and trace B (in water) exhibit monoexponential behavior of the decay with associated lifetimes of ∼360 ns in acetonitrile solution and ∼127 ns in aqueous solution, both of which are consistent with the previously reported lifetimes of ∼380 and 127 ns.[16,26] For the zeolite-entrapped complex, it was necessary to apply a biexponential model of the decay to reproduce the observed decay curve. This behavior arises for some other zeolite-entrapped complexes[9−14,33] because of the contribution from small fractions (∼6%) of interacting adjacent cage pairs.[34] The lifetime for the aqueous suspension of the zeolite-entrapped $Ru(bpy)_2(dpp)^{2+}$ complex was ∼90 ns with a second component (∼475 ns) contributing approximately

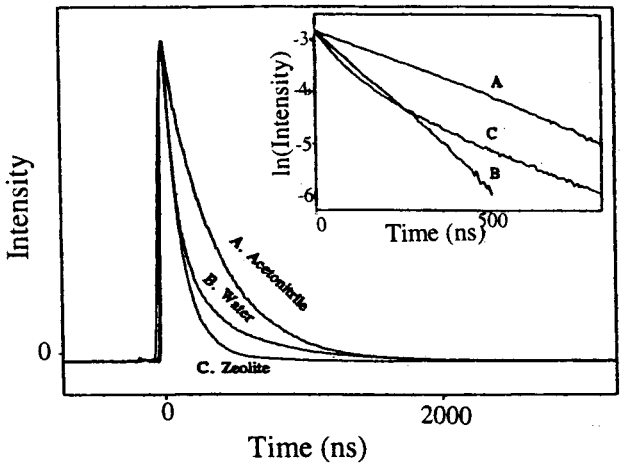

Figure 2. Emission decay curves of the $Ru(bpy)_2(dpp)^{2+}$ complex obtained at room temperature with 354.7 nm excitation: free complex in acetonitrile (trace A); free complex in water (trace B); zeolite-entrapped complex (trace C). The insert presents the logarithmic plots for the same data.

20% of the initial emission intensities. The minor component is attributable to the small fraction (less than 1%) of Z−$Ru(bpy)_3^{2+}$ impurity and (possibly) a small contribution from interacting adjacent cage pairs.[34] The minor component actually may represent an averaged contribution of Z−$Ru(bpy)_3^{2+}$ and adjacent cage pairs. The individual components cannot be resolved during the numerical fitting because of the small relative contribution to the emission decay. If the relative contribution of an emissive component decreases to ∼5%, then the error associated with the corresponding lifetime increases.[35] The lifetime of the zeolite-entrapped complex was measured at different monitoring wavelengths (600, 625, 650, and 700 nm) which yielded lifetimes consistent with the presence of a small amount of $Ru(bpy)_3^{2+}$ impurity (the intensity of the second component increases from 20% at 700 nm to 75% at 600 nm because the the $Ru(bpy)_3^{2+}$ impurity emits near 600 nm). The conclusion that the biexponential behavior results from the presence of a small amount of $Ru(bpy)_3^{2+}$ impurity, rather than

(33) Turbeville, W.; Robins, D. S.; Dutta, P. K. *J. Phys. Chem.* **1992**, *96*, 5024.

(34) Sykora, M.; Kincaid, J. R.; Dutta, P. K.; Castagnola, N. B. *J. Phys. Chem.* **1999**, *103*, 309.

(35) Sykora, M. Ph.D. Dissertation, Marquette University, Milwaukee, WI, 1997; pp 135.

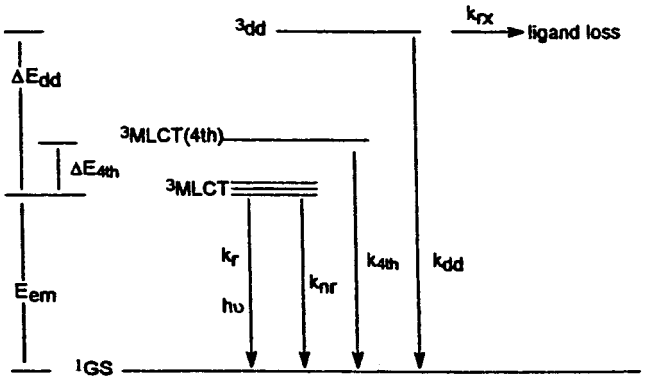

Figure 3. Schematic representation of the excited-state deactivation pathways in ruthenium polypyridine complexes.

(for example) different site locations of the targeted complex, is further supported by the fact that the luminescence decay curve of a solution of the HF extract of the zeolitic material also exhibited biexponential behavior with parameters consistent with those expected for a mixture of the two complexes (i.e., components having measured lifetimes of 133 and 480 ns at room temperature).

E. Temperature-Dependent Lifetimes. Ruthenium(II) polypyridine complexes relax to the ground state via a number of pathways, including population of two thermally accessible upper states, as is depicted in Figure 3. The extent of participation of these thermally accessible pathways can be documented by analysis of lifetime data acquired over a range of temperatures.[36−41] One thermally populated state, known as a ligand field (LF) state or ^{3}dd state, lies about 3500 cm^{-1} above the ^{3}MLCT state in the majority of complexes which have an accessible ^{3}dd state. In cases where the ^{3}dd state is not thermally accessible, population of another low lying ^{3}MLCT state (the so-called fourth MLCT state[42−44]) can make detectable contributions to the temperature-dependent decay curve as a consequence of a small energy gap (typically 600−900 cm^{-1}).[10,11,36−41]

For most complexes studied to date,[36−40] an expression involving a single thermal term (eq 1) is adequate to fit the experimental temperature-dependent lifetime data. However, in some cases,[10,11,41] it is necessary to use two thermal terms (eq 2) in order to fit the experimental data. The excited-state lifetimes (τ) are thus given by either

$$1/\tau = k_{total} = k_r + k_{nr} + k_{dd}\exp(-\Delta E_{dd}/k_B T) \qquad (1)$$

or

$$1/\tau = k_{total} = k_r + k_{nr} + k_{dd}\exp(-\Delta E_{dd}/k_B T) + k_{4th}\exp(-\Delta E_{4th}/k_B T) \qquad (2)$$

In eqs 1 and 2, τ is the lifetime, k_r and k_{nr} are the rate constants for radiative and nonradiative decay, k_{dd} is the deactivation rate constant of the thermally populated (^{3}dd) states, ΔE_{dd} is the energy gap between the ^{3}dd states and the ^{3}MLCT emitting states, k_{4th} is the deactivation rate constant of the fourth MLCT state, ΔE_{4th} is the energy gap between the ^{3}MLCT and fourth MLCT electronic excited states, and k_B is Boltzmann's constant.

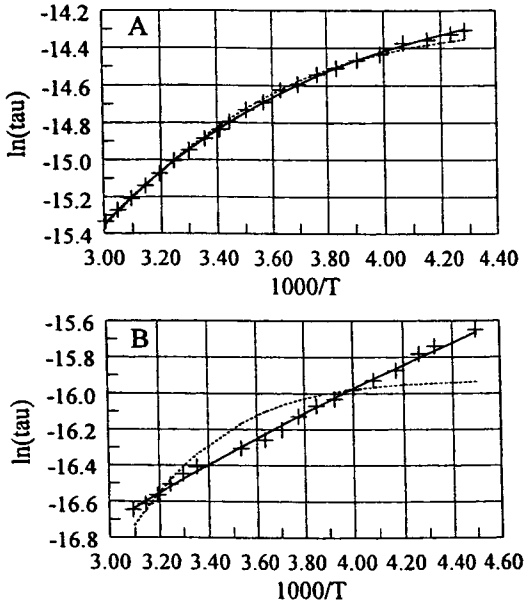

Figure 4. Temperature-dependent lifetime data obtained for the $Ru(bpy)_2(dpp)^{2+}$ free complex in acetonitrile (trace A) and the zeolite-entrapped complex (trace B). The experimental points are marked by crosses. The solid line was generated from eq 2 using two thermal terms; the dotted line was obtained from eq 1 with one thermal term.

Both equations were tested in an attempt to reproduce the observed lifetime data. Figure 4 presents the results of the fitting, both for the free complex in acetonitrile and for the zeolite-entrapped complex. Analysis of the curves shown in Figure 4 reveals that the single thermal term model does not satisfactorily reproduce the observed lifetime data but the introduction of the second thermal term yields excellent agreement between the calculated and observed curves. The short (major) component of the lifetimes was used for fitting of the temperature-dependent lifetimes and for calculation of the kinetic parameters. The parameters obtained for both of the thermal terms are quite similar to those obtained for many similar complexes.[10,11,36−41] Thus, the results obtained from this study indicate that, for the $Ru(bpy)_2(dpp)^{2+}$ complex, both states are thermally accessible and influence the lifetime. The kinetic parameters obtained from the analysis of the temperature-dependent lifetime data (including both thermal terms in the model) are shown in Table 2. Previous studies[9−13] have shown that, for ruthenium polypyridine complexes, there is a substantial increase in ΔE_{dd} upon zeolite entrapment, an effect which can lead to dramatic increases in lifetime and emission intensity for the zeolite entrapped complexes. In the present case, zeolite-entrapment does not have dramatic effects on the ^{3}MLCT state lifetime or the energy gaps between the low-lying ^{3}MLCT state and either of the thermally accessible states. In all previous cases studied, the entrapped tris-ligated complexes contained relatively small (two-ring) chelates, such as bipyridine and ligands of similar steric bulk.[10−14] Apparently, the greater steric bulk of the dpp ligand, with its appended (noncoordinated) pyridine fragment, leads to a slightly different orientation of the entrapped Ru-

(36) Allen, G. H.; White, R. P.; Rillema, D. P.; Meyer, T. J. *J. Am. Chem. Soc.* **1984**, *106*, 2613.
(37) Lumpkin, R. S.; Kober, M. E.; Worl, L. A.; Murtaza, Z.; Meyer, T. J. *J. Phys. Chem.* **1990**, *94*, 239.
(38) Rillema, D. P.; Blanton, C. B.; Shaer, R. J.; Jackman, D. C.; Boldaji, M.; Bundy, S.; Worl, L. A.; Meyer, T. J. *Inorg. Chem.* **1992**, *31*, 1600.
(39) Barqawi, K. R.; Llobet, A.; Meyer, T. J. *J. Am. Chem. Soc.* **1988**, *110*, 7751.
(40) Caspar, J. V.; Meyer, T. J. *Inorg. Chem.* **1983**, *22*, 2444.
(41) Sykora, M.; Kincaid, J. R. *Inorg. Chem.* **1995**, *34*, 5852.
(42) Yersin, H.; Gallhuber, E.; Vogler, A.; Kunkely, H. *J. Am. Chem. Soc.* **1983**, *105*, 4155.
(43) Yersin, H.; Gallhuber, E. *J. Am. Chem. Soc.* **1984**, *106*, 6582.
(44) Yersin, H.; Gallhuber, E.; Hensler, G. *Chem. Phys. Lett.* **1987**, *134*, 497.

Table 2. Kinetic Decay Parameters for the $Ru(bpy)_2(dpp)^{2+}$ Complex

complex	$k_r + k_{nr}$ (s^{-1})	k_{dd} (s^{-1})	ΔE_{dd} (cm^{-1})	k_{4th} (s^{-1})	ΔE_{4th} (cm^{-1})
$Ru(bpy)_2(dpp)(ClO_4)_2$[a] (in acetonitrile)	$(1.26 \pm 0.07) \times 10^6$	$(8.68 \pm 0.05) \times 10^{11}$	3230 ± 57	$(2.7 \pm 0.1) \times 10^8$	1075 ± 115
$Ru(bpy)_2(dpp)(ClO_4)_2$[b] (in acetonitrile)	$(1.58 \pm 0.03) \times 10^6$	$(4.9 \pm 1.2) \times 10^9$	1707 ± 58		
$Z-Ru(bpy)_2(dpp)^{2+}$ [a] (in zeolite)	$(2.0 \pm 0.2) \times 10^6$	$(7.8 \pm 0.2) \times 10^{11}$	3239 ± 69	$(2.0 \pm 0.2) \times 10^8$	593 ± 203
$Z-Ru(bpy)_2(dpp)^{2+}$ [b] (in zeolite)	$(8.3 \pm 0.3) \times 10^6$	$(4.9 \pm 1.0) \times 10^{11}$	2417 ± 51		

[a] Fitted using two thermal terms. [b] Fitted using one thermal term.

$(bpy)_2dpp^{2+}$complex, which causes a relaxation of the supercage constraints responsible for the normally encountered increase in ΔE_{dd}.

Conclusion

The present study summarizes an efficient synthetic method for the preparation of a zeolite-entrapped $Ru(bpy)_2(dpp)^{2+}$ complex. Spectroscopic and photophysical studies confirm the structural integrity of the complex and document the fact that its inherently favorable photophysical properties are not substantially altered by the zeolite framework. The substantial red shift in the emission maximum, observed upon entrapment, presumably arises because of sterically induced distortions of the bound dpp ligand. Analysis of the observed resonance Raman spectra, which consist of bpy and dpp vibrations, indicate that it is the dpp-based modes which experience the largest shifts upon entrapment. This material may be viewed as an attractive precursor for the construction of covalently linked intrazeolitic molecular assemblies.

Acknowledgment. This work was supported by a grant from the Division of Chemical Sciences, U.S. Department of Energy (Grant DE-FG02-86ER 13619).

IC990359S